UC Irvine
UC Irvine Previously Published Works

Title

Absence of REV3L promotes p53-regulated cancer cell metabolism in cisplatin-treated lung carcinoma cells

Permalink

Journal

ISSN

Authors

Kong, Linghao
Murata, Michael M
Digman, Michelle A

Publication Date

2018

DOI

Peer reviewed

Absence of REV3L promotes p53-regulated cancer cell metabolism in cisplatin-treated lung carcinoma cells

Linghao Kong[a,b,†], **Michael M. Murata**[a,†], and **Michelle A. Digman**[a,*]

[a]Laboratory for Fluorescence Dynamics, Department of Biomedical Engineering, University of California, Irvine, CA 92697, USA

[b]University High School, Irvine, CA 92612, USA

Abstract

Lung cancer is one of the deadliest cancers in the world because of chemo-resistance to the commonly used cisplatin-based treatments. The use of low fidelity DNA polymerases in the translesional synthesis (TLS) DNA damage response pathway that repairs lesions caused by cisplatin also presents a mutational carcinogenic burden on cells that needs to be regulated by the tumor suppressor protein p53. However, there is much debate over the roles of the reversionless 3-like (REV3L) protein responsible for TLS and p53 in regulating cancer cell metabolism. In this study, the fluorescence lifetime of the metabolic coenzyme NADH reveals that the absence of REV3L can promote the p53-mediated upregulation of oxidative phosphorylation in cisplatin-treated H1299 lung carcinoma cells and increases cancer cell sensitivity to this platinum-based chemotherapy. These results demonstrate a previously unrecognized relationship between p53 and REV3L in cancer cell metabolism and may lead to improvements in chemotherapy treatment plans that reduce cisplatin resistance in lung cancer.

Keywords

Introduction

Lung carcinoma is one of the deadliest cancers in the world [1]. Cisplatin-based combination chemotherapy is one of the most common methods for managing and treating lung cancer. Cisplatin reduces cancer cell proliferation by creating DNA crosslinks that stall replication forks, which are highly toxic to rapidly dividing cells. The covalent bonds formed at these crosslinks inhibit motion of DNA polymerases at replication forks, forcing the polymerases to be ejected from the DNA strand [2]. These DNA adducts initiate the

DNA damage response (DDR), activating the tumor suppressor protein p53. Activation of p53 leads to processes that regulate metabolism, limit proliferation, and resist carcinogenesis [3]. Accumulation of cisplatin adducts repeatedly activates DNA damage signaling, which reduces cyclin-dependent kinase activity leading to cell cycle arrest [4].

Patients typically have favorable initial responses to cisplatin-based regimens, but these are brief and offer only marginal improvement due to the development of chemotherapy-resistance. Several mechanisms of resistance have been proposed, including changes in DNA methylation, alterations of membrane protein trafficking, and increased DNA repair [5]. In particular, the activation of DNA damage responses at DNA lesions such as cisplatin-induced crosslinks prevent replication fork collapse and promote survival, eventually leading to cisplatin resistance [6]. These bulky DNA lesions are processed by translesional DNA synthesis (TLS) and mediated by specialized DNA polymerases, such as Pol ζ. Unlike the highly accurate DNA polymerases used in replication, such as Pol δ, Pol ζ has low fidelity nucleotide insertion. The reversionless 3-like (REV3L) protein is the catalytic subunit of Pol ζ that is responsible for TLS [7]. REV3L has been shown to increase cancer cell viability, especially following cisplatin-induced damage [8–10].

The use of low fidelity DNA polymerases in TLS presents a mutational carcinogenic burden on cells that needs to be regulated by the tumor suppressor protein p53. In addition to suppressing TLS, p53 has many key functions in resisting carcinogenesis including cell cycle arrest, apoptosis, and metabolic regulation. Without p53, cancer cells can proceed with high rates of unregulated glycolysis, known as the Warburg effect and is one of the hallmarks of cancer [11]. This p53-mediated regulation of metabolism occurs through its promotion of target genes such as glutaminase 2 and TIGAR to upregulate oxphos and down-regulate glycolysis, respectively [12]. Furthermore, REV3L may also be involved in metabolic regulation, but its effects on metabolism are still debated with some studies suggesting that REV3L increases reliance on glycolysis and others demonstrating that it promotes oxphos [9, 13]. Because the one of the hallmarks of cancer cells is Warburg metabolism, understanding the mechanisms that limit the cancerous metabolic phenotype may lead to improvements in chemotherapy treatment plans that reduce cisplatin resistance in cancer cells. Indeed, the expression of p53 in p53-null cisplatin-resistant cell lines has been shown to increase sensitivity to cisplatin [14]. In this study, the absence of REV3L can promote the p53-mediated upregulation of oxphos in cisplatin-treated H1299 lung carcinoma cells and increases cancer cell sensitivity to this platinum-based chemotherapy.

Materials and Methods

Cell Culture, Plasmids, Transfections, and Treatments

H1299 cells (ATCC) were cultured in RPMI (Invitrogen, Carlsbad, CA) supplemented with 10% fetal bovine serum (FBS) and 1% penicillin-streptomycin. Cells were trypsinized and plated at 60–80% confluency on a glass-bottomed imaging dish. The EGFP and p53-GFP plasmids are commercially available through Addgene while the p53-R175H-GFP plasmid was kindly constructed and provided by Dr. Lee Bardwell and Dr. Jane Bardwell in the Department of Developmental and Cell Biology at the University of California, Irvine. Lipofectamine 3000 (Invitrogen, Carlsbad, CA) was used to transfect according to

manufacturer's instructions. Cells were incubated at 37°C and 5% CO_2 for 12–24 hours prior to imaging. To induce intra-strand crosslinks, cells were treated with 20 μM cis-diamminedichloroplatinum (II) (cisplatin) (Sigma-Aldrich, St. Louis, MO) for the duration of the experiments. For inhibition of oxidative phosphorylation, cells were treated with 10 μM rotenone and 10 μM antimycin A (Sigma-Aldrich, St. Louis, MO) in 0.35% DMSO for 1 hour prior to imaging. For inhibition of glycolysis, cells were treated with 20 mM 2-deoxy-D-glucose and 5 mM dichloroacetate (Sigma-Aldrich, St. Louis, MO) for 6 hours prior to imaging.

shRNA, siRNA, and Western Blot

Short hairpin RNA (shRNA) against REV3L (shREV3L) (pSuperior.puro-shREV3-4, Addgene #38029) and short interfering RNA (siRNA) against REV3L (siREV3L) (UrCUrGrGrCrGrCUrGUrCrArArGUUCTT) were used to silence the *REV3L* gene. The shRNA control (shControl) is commercially available at Sigma and the siRNA control (siControl) is commercially available at QIAGEN. Transfections of shRNA and siRNA were done following DNA plasmid transfection but had identical steps, with shRNA or siRNA in lieu of the DNA plasmid. 1 μg of shRNA or 1 μL of 20 μM siRNA was used for the transfection of each imaging dish. 24 hours after shRNA transfection, 2.0 μg/mL puromycin RPMI 1640 media was applied for 24 hours to select for successfully transfected shRNA cells. Cells were harvested for Western blot analysis or imaged approximately 24 hours after the final transfection. Whole cell lysates prepared with RIPA buffer were subjected to SDS-PAGE followed by Western blot analysis with the anti-REV3L antibody (MyBioSource) and the anti-β tubulin antibody (Sigma-Aldrich, St. Louis, MO) for the loading control.

Instrumentation and Data Analysis

Confocal and fluorescence lifetime imaging microscopy (FLIM) experiments were performed on an inverted confocal Zeiss LSM710 (Carl Zeiss, Jena, Germany) with a 40x 1.2NA water-immersion objective (Zeiss, Korr C-Apochromat). Green fluorescent protein (GFP) excitation was achieved using a one-photon argon ion laser at 488 nm and emission was captured at 500–600 nm. In FLIM experiments, a Mai Tai titanium-sapphire 100 femto-second pulsed laser at 80 MHz (Spectra-Physics, Santa Clara, CA) was used for sample excitation. An ISS A320 FastFLIM box (ISS, Champaign, IL) and a photomultiplier tube (H7422P-40, Hamamatsu Photonics, Hamamatsu, Japan) were used for data acquisition. FLIM images were acquired at 740 nm two-photon excitation with image sizes of 256×256 pixels and a scan speed of 25.21 μs/pixel. Fluorescence signal was captured at 420–500 nm for NADH auto-fluorescence. Instrument response time was referenced using coumarin-6 in pure ethanol, which has a known single exponential lifetime of 2.5 ns. FLIM data was processed in the SimFCS software developed at the Laboratory for Fluorescence Dynamics, University of California, Irvine as previously described [15].

Cell Viability Assay

Cells were plated onto gridded imaging dishes to determine cell survival following cisplatin treatment using morphology. Cell viability was measured by vital dye exclusion by propidium iodide (0.8 μg/mL) and total cell count was determined by Hoechst 33342 (0.5 μg/mL).

Results

p53 upregulates oxidative phosphorylation in H1299 cells

The tumor suppressor p53 has been known to regulate metabolism through the upregulation of oxphos and the downregulation of glycolysis. In some situations, however, it has also been known to upregulate glycolysis [3]. We first sought to elucidate the impact of p53 on the fraction of protein-bound NADH in H1299 cancer cells, which can be indicative of the overall metabolic state of the cell. The p53-null H1299 lung carcinoma cells were transfected with wild type p53 (p53-GFP) or the EGFP control. Fluorescence lifetime data of NADH in H1299 cells was acquired to observe changes in the fraction of bound NADH. Previous studies have demonstrated that the phasor approach to fluorescence lifetime analysis provides a graphical representation of lifetime data and by using 740 nm excitation with a bandpass filter, the fluorescence signal from NADH can be isolated. Here, FLIM data of NADH was collected and transformed to coordinates on the phasor plot as previously described (Figure 1A) [15]. Once the phasor positions of freely floating NADH and protein-bound NADH are established, the fraction of bound NADH can be determined by the linear combination of the phasors, which follow the rules of vector addition [16]. Images were pseudo-colored based on the fluorescence lifetime along this linear combinatorial trajectory with shorter lifetimes colored red and longer lifetimes colored white to illustrate free and bound NADH, respectively. Brightfield images for both EGFP and p53-GFP cells were taken to demonstrate the nuclear localization of p53 (Figure 1B). Pseudo-colored FLIM images of H1299 cells shows the sub-cellular distribution of NADH and that p53 induces a shift toward bound NADH in the cytoplasmic and nuclear compartments. H1299 cells expressing p53 exhibited a significantly higher fraction of bound NADH relative to control p53-null cells. This difference was observed in both the nuclear and the cytoplasmic sub-cellular compartments (Figure 1C).

To determine whether or not the fraction of bound NADH reflects the cellular metabolic state of H1299 cells, combinations of mitochondrial and glycolytic inhibitors were used as demonstrated previously [17]. For inhibition of mitochondrial oxidative phosphorylation, 10 μM rotenone and 10 μM antimycin A (R+AA) were used to disrupt the electron transport chain at the NADH dehydrogenase and coenzyme Q – cytochrome c reductase, respectively. To inhibit glycolysis, 20 mM 2-deoxy-D-glucose and 5 mM dichloroacetate (DG+DCA) were used to prevent the processing of glucose and to increase pyruvate intake for mitochondrial respiration. Following R+AA treatment, there was a highly significant percent decrease in the bound fraction of NADH relative to basal levels suggesting that a high fraction of bound NADH reflects increased oxidative phosphorylation relative to glycolysis (Figure 1D). Following DG+DCA treatment, there was a highly significant percent increase of the fraction of bound NADH for cells treated with DG+DCA relative to basal levels while control cells exhibited no significant changes in the fraction of bound NADH. Thus, for H1299 cells, a higher fraction of bound NADH corresponds to increased rates of oxidative phosphorylation relative to glycolysis, which is consist with previous studies linking the lifetime of NADH to energy metabolism [16]. Together, the data suggest that investigating the fraction of bound NADH by FLIM can describe cellular metabolism and that p53 upregulates oxidative phosphorylation in H1299 cells.

REV3L is necessary for p53 metabolic regulation

Previous studies suggest that REV3L may have an impact on glycolysis and oxphos in cancer cells, but its effects are still debated [9, 13]. To investigate the effect of REV3L and p53 on cellular metabolism, p53-null H1299 cells and H1299 cells expressing p53 were depleted of REV3L via short hairpin RNA (Supplemental Figure 1). Depletion of REV3L in p53-null H1299 cells did not significantly change the fraction of bound NADH relative to control cells (Figure 2A). The expression of p53 in H1299 cells exhibited an increase in the fraction of protein-bound NADH relative to p53-null control cells, demonstrating the upregulation of oxphos by p53 as in Figure 1C. The depletion of REV3L by shRNA in p53-expressing cells, however, caused a significant decrease in the fraction of bound NADH relative to cells with functional REV3L. The decrease in protein-bound NADH suggests that oxphos is suppressed in the REV3L-depleted and p53-expressing H1299 cells relative to REV3L-expressing and p53-expressing cells demonstrating that REV3L is involved in metabolic regulation by p53. To investigate the effect of mutated p53 as commonly found in cancers, p53 with the R175H hotspot mutation (p53 mut) was expressed in H1299 cells and REV3L was depleted via small interfering RNA. As in Figure 2A, the fraction of bound NADH was not significantly affected by siREV3L alone, but increased with the expression of wild type p53 (Figure 2B). Depletion of REV3L in wild-type p53-expressing cells exhibited a decrease in the fraction of protein bound NADH suggesting that REV3L is necessary for the upregulation of oxphos by p53. Together, the results demonstrate a link between REV3L and p53 in regulating cellular metabolism in H1299 cells.

p53 maintains oxphos in response to cisplatin-induced DNA damage

The role of p53 in response to cisplatin-induced DNA damage is still debated with some studies suggesting p53 suppresses apoptosis while others demonstrating it promotes apoptosis [18]. Here, we investigate cellular metabolism via the fraction of bound NADH in p53-null H1299 cells and p53-expressing H1299 cells continuously treated with cisplatin for 12 hours. The fraction of bound NADH in both the nucleus and cytoplasm of p53-null H1299 cells exhibited significant decreases after treatment with cisplatin for 12 hours, indicating a decrease in oxphos (Figure 2C). However, the bound NADH fraction in both the nucleus and cytoplasm of H1299 cells expressing p53 did not change significantly with 12 hours of exposure to cisplatin. The high fraction of bound NADH in cisplatin-treated cells expressing p53 suggests that p53 regulates metabolism in the DNA damage response by maintaining a higher rate of oxphos than glycolysis relative to that in p53-null control cells.

The absence of REV3L increases p53-regulated oxphos following cisplatin treatment

Since REV3L appeared to affect basal p53-regulated metabolism, we investigated the metabolic response of H1299 cells in cisplatin-treated cells expressing p53 with REV3L depletion by shRNA. The significant positive percent change in the fraction of bound NADH after 24 hours of treatment by cisplatin from basal suggests an increase of p53-regulated metabolism in the absence of REV3L (Figure 3A). Depletion of REV3L or expression of p53 alone did not exhibit positive percent changes in the fraction of bound NADH with cisplatin treatment. Using the p53-R175H mutant with siRNA depletion of REV3L exhibited similar percent change increases with cisplatin (Figure 3B). The percent increase in the

bound fraction of NADH was greatest for cells expressing p53 with REV3L depletion via siRNA following cisplatin-induced DNA damage. Depletion of REV3L or expression of p53 alone also exhibited significant positive percent changes in the fraction of bound NADH after 24 hours of exposure to cisplatin, but not as great as that with the combination of p53 expression and REV3L depletion. The FLIM results suggest that there is a significant enhancement of p53-regulated oxphos as a result of cisplatin treatment in the absence of REV3L.

Cancer cell sensitivity to cisplatin increases with p53 expression and REV3L depletion

Because cancer cells generally exhibit high rates of glycolysis, we aimed to determine whether or not the p53-enhanced oxphos when REV3L is depleted increased cancer cell sensitivity to cisplatin treatment. Cell survival was determined by morphology and a live/dead assay with Hoechst 33342 and propidium iodide (Figure 4A). The survival rate of H1299 cells at 24 hours with cisplatin treatment was determined by subtracting the number of cells uptaking propidium iodide from the initial number of cells and normalizing for the number of cells in the field of view (Figure 4B). Expression of p53 in the absence of REV3L exhibited a lower survival rate for H1299 cells relative to REV3L depletion or expression of p53 alone as well as the control showing that cancer cell sensitivity to cisplatin increases with p53 expression and REV3L depletion.

Discussion

The study herein suggests that the absence of REV3L can promote the p53-mediated upregulation of oxphos in H1299 lung carcinoma cells treated with cisplatin and increases cancer cell sensitivity to the cisplatin treatment. By measuring the fluorescence lifetime of NADH and calculating the fraction of protein-bound NADH throughout the cell, it was observed that cancer cells lacking REV3L but expressing functional p53 exhibit higher rates of oxidative phosphorylation than cells lacking REV3L or expressing p53 alone. Without REV3L, TLS and the subsequent repair of cisplatin-induced DNA lesions is greatly reduced and DNA damage signaling can persist. Furthermore, p53 halts the cell cycle until repair is completed and mediates the upregulation of oxphos, thereby antagonizing the cancerous metabolic phenotype characterized by high rates of glycolysis. These cancer cells then exhibited increased sensitivity to cisplatin treatment relative to cells only lacking REV3L, only expressing wild type p53, and control cells. A model for the roles of REV3L and p53 in lung cancer sensitivity to cisplatin is proposed (Figure 4C). This presents a promising area for future development of treatment plans that can address lung cancer resistance to cisplatin.

We observed an increased fraction of bound NADH in the absence of REV3L even without p53 activity. Other DNA damage signaling events, namely PARP activity, which consumes NAD+ and inhibits glycolysis, can cause an overall cellular increase of bound NADH [19]. Thus, depleting REV3L in cells that lack functional p53 can still initiate the DDR leading to other signaling cascades that can suppress the cancerous metabolic phenotype and ultimately reduce cancer cell proliferation. While the observed survival rate following cisplatin treatment in H1299 cells lacking both REV3L and functional p53 was comparable to wild

type H1299 cells, it is worth investigating treatments that target REV3L in order to reduce resistance to cisplatin.

In this study, p53-null H1299 lung carcinoma cells were used. The introduction of functional p53 into H1299 cancer cells confers the tumor suppressive properties of p53, including metabolic regulation, which were previously not present. In basal conditions, p53 promotes oxphos and inhibits glycolysis [20]. Thus, the higher bound NADH fraction as measured by FLIM in H1299 cells expressing p53 relative to control cells is consistent with previous research. The increased sensitivity to cisplatin treatment in cells expressing both functional p53 and REV3L could occur due to the initiation of multiple DNA repair pathways such as the REV3L-mediated TLS and the ATR signaling pathway [21]. ATR signaling to p53 can increase oxphos, therefore increasing the fraction of bound NADH. Restoring p53, then, in cancer cells lacking functional p53 or expressing mutated p53 presents a very promising option for co-treatment with cisplatin chemotherapy.

The metabolic regulatory functions of p53 have only been recently discovered within the past few decades while the role of REV3L in metabolism is still currently unclear. This study provides some insight into the role of REV3L in metabolism and its interaction with the tumor suppressor p53 in that REV3L appears necessary for p53-mediated upregulation of oxphos. The data show a previously unidentified connection between p53 and REV3L in regulating metabolism and require further research to better understand the underlying interactions between them in this fight against chemotherapeutic resistance.

Supplementary Material

Refer to Web version on PubMed Central for supplementary material.

Acknowledgments

Abbreviations

REV3L	reversionless-3 like
TLS	translesional DNA synthesis
FLIM	fluorescence lifetime imaging and microscopy
NADH	reduced nicotinamide adenine dinucleotide
Oxphos	oxidative phosphorylation
R+AA	rotenone and antimycin A
DG+DCA	2-deoxy-D-gluocose and dichloroacetate

| **DDR** | DNA damage response |

References

1. Ferlay J, et al. Cancer incidence and mortality worldwide: sources, methods and major patterns in GLOBOCAN 2012. Int J Cancer. 2015; 136(5):E359–86. [PubMed: 25220842]

2. Dasari S, Tchounwou PB. Cisplatin in cancer therapy: molecular mechanisms of action. Eur J Pharmacol. 2014; 740:364–78. [PubMed: 25058905]

3. Zilfou JT, Lowe SW. Tumor suppressive functions of p53. Cold Spring Harb Perspect Biol. 2009; 1(5):a001883. [PubMed: 20066118]

4. Jackson SP, Bartek J. The DNA-damage response in human biology and disease. Nature. 2009; 461(7267):1071–8. [PubMed: 19847258]

5. Shen DW, et al. Cisplatin resistance: a cellular self-defense mechanism resulting from multiple epigenetic and genetic changes. Pharmacol Rev. 2012; 64(3):706–21. [PubMed: 22659329]

6. Waters LS, et al. Eukaryotic translesion polymerases and their roles and regulation in DNA damage tolerance. Microbiol Mol Biol Rev. 2009; 73(1):134–54. [PubMed: 19258535]

7. Gan GN, et al. DNA polymerase zeta (pol zeta) in higher eukaryotes. Cell Res. 2008; 18(1):174–83. [PubMed: 18157155]

8. Wang W, et al. REV3L modulates cisplatin sensitivity of non-small cell lung cancer H1299 cells. Oncol Rep. 2015; 34(3):1460–8. [PubMed: 26165320]

9. Singh B, et al. Human REV3 DNA Polymerase Zeta Localizes to Mitochondria and Protects the Mitochondrial Genome. PLoS One. 2015; 10(10):e0140409. [PubMed: 26462070]

10. Knobel PA, et al. Inhibition of REV3 Expression Induces Persistent DNA Damage and Growth Arrest in Cancer Cells. Neoplasia. 2011; 13(10):961–IN28. [PubMed: 22028621]

11. Warburg O, Wind F, Negelein E. The metabolism of tumors in the body. J Gen Physiol. 1927

12. Puzio-Kuter AM. The Role of p53 in Metabolic Regulation. Genes Cancer. 2011; 2(4):385–91. [PubMed: 21779507]

13. Sullivan EJ. Metabolic Changes Associated with Acquired Cisplatin Resistance. Open Access Dissertations. 2014:1192.

14. Chappell WH, et al. p53 expression controls prostate cancer sensitivity to chemotherapy and the MDM2 inhibitor Nutlin-3. Cell Cycle. 2012; 11(24):4579–88. [PubMed: 23187804]

15. Digman MA, et al. The phasor approach to fluorescence lifetime imaging analysis. Biophys J. 2008; 94(2):L14–6. [PubMed: 17981902]

16. Stringari C, et al. Phasor fluorescence lifetime microscopy of free and protein-bound NADH reveals neural stem cell differentiation potential. PLoS One. 2012; 7(11):e48014. [PubMed: 23144844]

17. Fath MA, et al. Mitochondrial electron transport chain blockers enhance 2-deoxyD-glucose induced oxidative stress and cell killing in human colon carcinoma cells. Cancer Biol Ther. 2009; 8(13):1228–1236. [PubMed: 19411865]

18. di Pietro A, et al. Pro- and anti-apoptotic effects of p53 in cisplatin-treated human testicular cancer are cell context-dependent. Cell Cycle. 2012; 11(24):4552–62. [PubMed: 23165211]

19. Andrabi SA, et al. Poly(ADP-ribose) polymerase-dependent energy depletion occurs through inhibition of glycolysis. PNAS. 2014; 111(28):10209–10214. [PubMed: 24987120]

20. Shen L, et al. The fundamental role of the p53 pathway in tumor metabolism and its implication in tumor therapy. Clin Cancer Res. 2012; 18(6):1561–7. [PubMed: 22307140]

21. Caldon CE. Estrogen signaling and the DNA damage response in hormone dependent breast cancers. Front Oncol. 2014; 4:106. [PubMed: 24860786]

Highlights

- p53 upregulates oxidative phosphorylation in H1299 cells

- REV3L is necessary for p53 metabolic regulation

- p53 maintains oxphos in response to cisplatin-induced DNA damage

- The absence of REV3L increases p53-regulated oxphos following cisplatin treatment

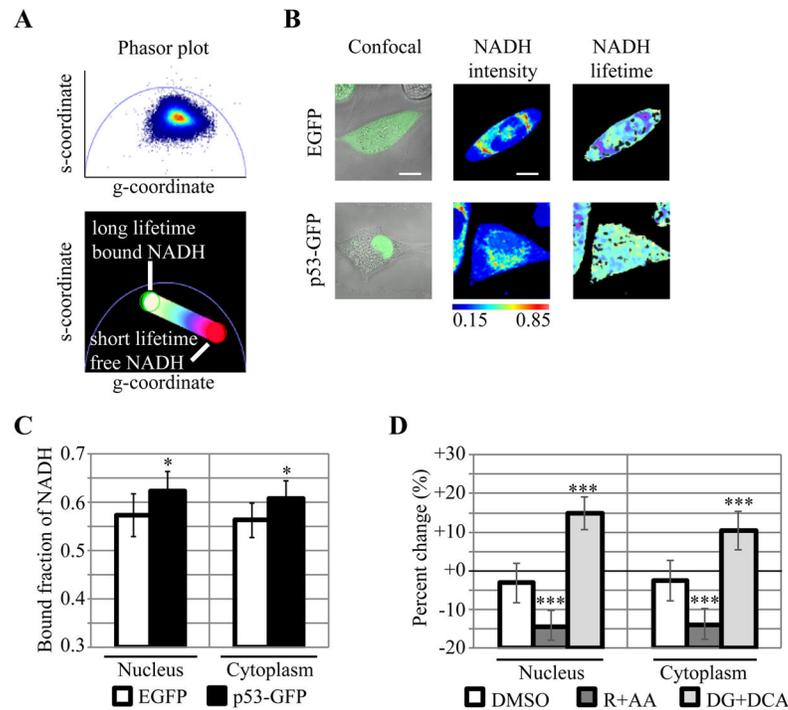- Cell sensitivity to cisplatin increases with p53 expression and REV3L depletion

Figure 1. p53 promotes oxidative phosphorylation
(A) The fluorescence lifetime histogram on the phasor plot shows the distribution of lifetimes of autofluorescent NADH. A color spectrum indicates the bound fraction of NADH. (B) Fluorescence intensity images of GFP of an EGFP cell and p53-GFP cell (left panels). Normalized fluorescence intensity images of NADH (middle panels) and pseudo-colored FLIM images (right panels) of H1299 lung cancer cells transfected with EGFP and p53-GFP. Pseudo-coloring corresponds to the phasor position according to the color spectrum in Figure 1A. Scale bar = 10μm. (C) Bar graphs quantifying the bound fraction of NADH in the nucleus (left) and cytoplasm (right). (D) Percent change in bound fraction of NADH in the nucleus (left) and cytoplasm (right) after treatment with DMSO, rotenone and antimycin A (R+AA), or 2-deoxy-D-glucose and dichloroacetate (DG+DCA).
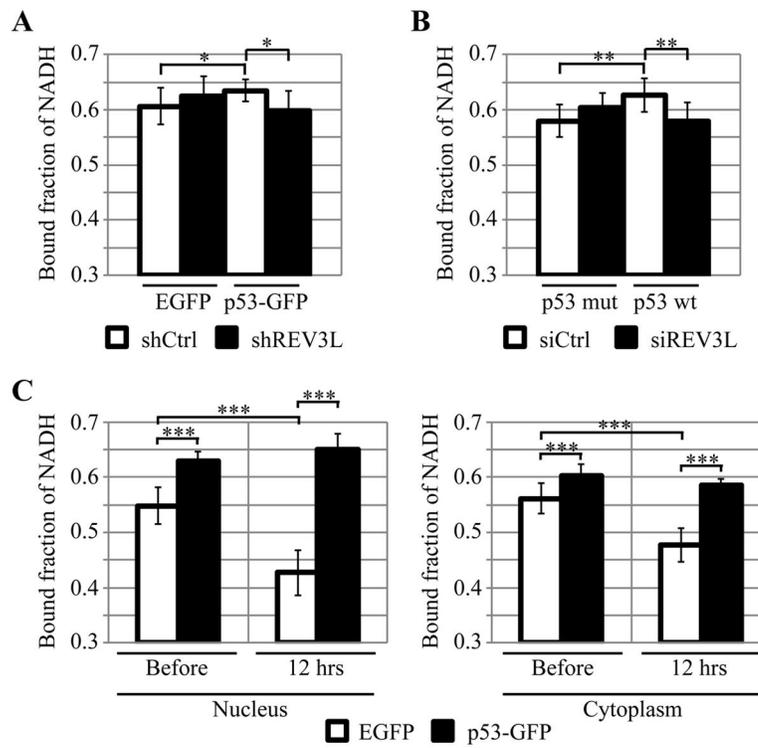* $p < 0.05$, *** $p < 0.001$, N>7.

Figure 2. REV3L is necessary for metabolic regulation by p53

(A) The fraction of bound NADH in H1299 cells after manipulation of p53 by transfection and REV3L by shRNA. (B) The fraction of bound NADH after transfection of wild type p53-GFP (p53 wt) or p53-GFP with the R175H mutation (p53 mut) and depletion of REV3L by siRNA. (C) The fraction of bound NADH before cisplatin treatment and with 12 hours of continuous exposure to cisplatin in the nucleus (left) and in the cytoplasm (right).

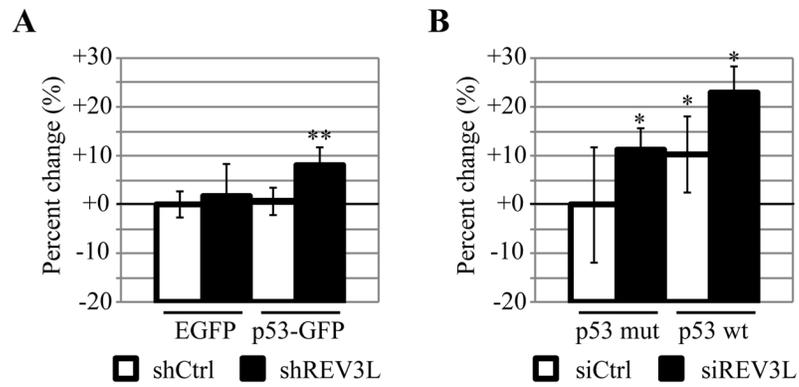$*$ $p<0.05$, $**$ $p<0.01$, $***$ $p<0.001$, $N>7$.

Figure 3. The absence of REV3L increases p53-regulated oxphos following cisplatin treatment
(A) The percent change in the fraction of bound NADH after manipulation of p53 by transfection and REV3L by shRNA with 24 hours of 20μM cisplatin treatment. (B) The percent change in the fraction of bound NADH after transfection of p53-GFP with the R175H mutation and depletion of REV3L by siRNA with 24 hours of 20μM cisplatin treatment.
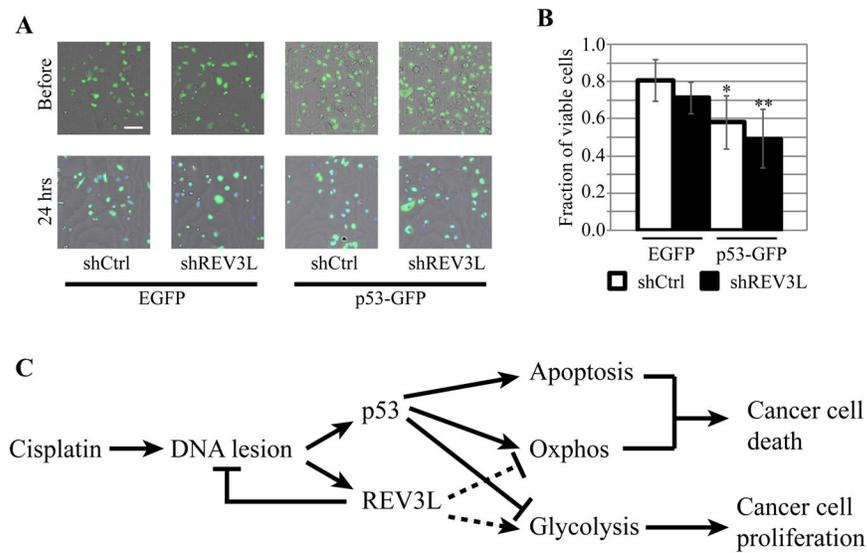
* $p<0.05$, ** $p<0.01$, N>7.

Figure 4. Cancer cell sensitivity to cisplatin increases with p53 expression and REV3L depletion
(A) Brightfield images of cells after manipulation of p53 by transfection and REV3L by shRNA with 24 hours of 20μM cisplatin treatment. Scale bar = 10μm. (B) Bar graph of the cell survival rate of H1299 cells. (C) A proposed model for the role of REV3L and p53 in cancer cell sensitivity to cisplatin. * p<0.05, ** p<0.01.